Experimental Evidence for Delocalization of the Lone-Pair Orbital in CH_3NH_2 from (e,2e) Spectroscopy

J. A. Tossell,*† S. M. Lederman,† J. H. Moore,† M. A. Coplan,‡ and D. J. Chornay‡

Contribution from the Department of Chemistry and Institute for Physical Science and Technology, University of Maryland, College Park, MD 20742. *Received June 30, 1983*

Abstract: Momentum distributions, $\rho(q)$, are obtained for the predominantly N 2p lone-pair orbitals of NH_3 and CH_3NH_2 by (e,2e) spectroscopy. SCF-MO calculations at the split valence level reproduce the shift in the position of the maximum of the momentum density in CH_2NH_2 relative to NH_3. However, as previously observed by Hood et al.,[6a] the observed position of the maximum for NH_3 is considerably different from that calculated for a wave function near the Hartree-Fock limit. Fourier transformation of $\rho(q)$ yields the wave function autocorrelations, $B(r)$, whose change from NH_3 to CH_3NH_2 may be understood by using contour plots of the average and difference of the position space orbital amplitudes. The lone-pair orbital of CH_3NH_2 is shown to possess a significant contribution from the methyl H trans to the major lobe of the lone pair, consistent both with qualitative perturbational MO theory and with the interaction energy decomposition analysis of Umeyama and Morokuma.[14d]

The representation of many-electron molecular wave functions in terms of orbitals is an extremely useful approximation for interpreting a wide variety of chemical data.[1] General methods have been developed to explain molecular shapes[2] and chemical reactivities[3] using information about orbital energies and orbital electron distributions. While experimental data on orbital energies can be obtained from photoelectron spectroscopy,[4] experimental determination of orbital character and electron distributions has been more difficult to obtain. In the last few years a new technique, (e,2e) spectroscopy,[5] has begun to yield information about the distribution of momenta in individual electron orbitals. The technique is based on high-energy electron impact ionization with complete determination of the collision kinematics.

In principle, there is a great deal of information about electronic structure in the experimental momentum distributions obtainable from (e,2e) spectroscopy. Because of experimental difficulties and the lack of a suitable method for extracting this information, most (e,2e) studies of the electronic structure of atoms and molecules have concentrated on comparisons between the experimental momentum distributions and calculated distributions based on theoretical wave functions. In an effort to further probe the potential of the (e,2e) techniques we have chosen the lone-pair orbitals in two similar molecules, NH_3 and CH_3NH_2. They present an interesting system because their chemical properties appear to be closely related to the lone-pair electrons and there exist a number of theoretical studies of their molecular wave functions. Furthermore, previous studies of the momentum distribution of the lone-pair orbitals of NH_3 by Hood et al.[6a] and Camilloni et al.[6b] showed a distinct discrepancy between theory and experiment. By a comparative study of two similar molecules we emphasize their chemically interesting differences.

The cross section for the (e,2e) process simplifies to the product of a collision term and a structure term if the incident, scattered, and knocked-out electrons can be represented as plane waves and the binary encounter approximation is used. Furthermore, if the bound-state total wave function can be written as a single configuration antisymmetrized product of one-electron orbitals ψ_i,

$$\Psi = \hat{A}\prod_i \psi_i \tag{1}$$

the (e,2e) cross section reduces to

$$\sigma_{(e,2e)} \propto \sigma_{(e,e)}|\langle e^{i\vec{q}\cdot\vec{r}}|\psi_k(\vec{r})\rangle|^2 \tag{2}$$

where $\sigma_{(e,e)}$ is the electron-electron scattering cross section and the term in brackets is the Fourier transform of the wave function for the orbital from which the knocked-out electron has been removed. The transform is equivalent to the momentum space wave function $\phi(\vec{q})$, and its square modulus is the momentum distribution $\rho(\vec{q})$ (more complete treatments of the theory are given in ref 5).

Because $\psi(\vec{r})$ and $\phi(\vec{q})$ are equivalent representations, they have the same symmetry properties. In addition there is the well-known inverse relationship between the amplitudes of the two functions: an orbital that is compact in one space is diffuse in the other and vice versa. Similarly, the amplitude of $\rho(\vec{q})$ at small $\vec{q}$ is related most directly to the amplitude of $\rho(\vec{r})$ at large $\vec{r}$.

Momentum distributions can be converted to the position space function $B(\vec{r})$ via a Fourier transform[7]

$$B(\vec{r}) = \frac{1}{(2\pi)^{3/2}}\int \rho(\vec{q})e^{i\vec{q}\cdot\vec{r}}\,d\vec{q} \tag{3}$$

which is equivalent to the autocorrelation of the position space wave function

$$B(\vec{r}) = \int \psi(\vec{s})\psi(\vec{s}+\vec{r})\,d\vec{s} \tag{4}$$

The function $B(\vec{r})$ is the position space analogue of the well-known momentum space X-ray diffraction form factor $F(\vec{q})$ which itself is the Fourier transform of the charge distribution. Though $\rho(\vec{q})$ and $B(\vec{r})$ contain the same information, the usefulness of $B(\vec{r})$ comes from our habit of thinking in position space rather that momentum space and from the important practical point that the spherical average of $B(\vec{r})$ can be obtained in a routine manner from experimentally measured, spherically averaged, momentum distributions.[5,8] While it is true that spherical averaging reduces information content, sufficient detail remains in the spherically averaged function $B(r)$ to make it useful in interpreting a wide range of theoretical and experimental data. Most analyses of (e,2e) momentum distributions have been based on general discussions of the shapes of $\rho(q)$. Through the $B(r)$ function more quantitative comparisons between experiment and theory are possible. Weyrich et al.[9] have discussed the use of the $B(\vec{r})$ function for the investigation of the electronic structure of atoms and molecules, and in a recent paper we have shown that differences between the orbitals of CO, NO, and O_2 can be observed

† Department of Chemistry.
‡ Institute for Physical Science and Technology.

(1) K. Wittel and S. P. McGlynn, *Chem. Rev.*, **77**, 745, (1977).
(2) J. K. Burdett, "Molecular Shapes: Theoretical Models of Inorganic Stereochemistry", Wiley-Interscience, New York, 1980.
(3) G. Klopman, Ed., "Chemical Reactivity and Reaction Paths", Wiley, New York, 1974.
(4) D. W. Turner, C. Baker, A. D. Baker, and C. R. Brundle, "Molecular Photoelectron Spectroscopy: A Handbook of the 584 A Spectra", Wiley-Interscience, New York, 1970.
(5) J. H. Moore, J. A. Tossell, and M. A. Coplan, *Acc. Chem. Res.*, **15**, 1982 (1982); I. E. McCarthy and E. Weigold, *Phys. Rep.*, **27**, 275 (1976).
(6) (a) S. Hood, A. Hammett, and C. E. Brion, *Chem. Phys. Lett.*, **39**, 252 (1976); (b) R. Camilloni, G. Stefani, A. Giardini-Guidoni, R. Tiribelli, and D. Vinciguerra, *Chem. Phys. Lett.*, **41**, 17 (1976).
(7) R. Benesch, S. R. Singh, and V. H. Smith, Jr., *Chem. Phys. Lett*, **10**, 151 (1971).
(8) J. A. Tossell, J. H. Moore, and M. A. Coplan, J. *Electron Spectrosc. Relat. Phenom.*, **22**, 61 (1981).
(9) W. Weyrich, P. Pattison, and B. G. Williams, *Chem. Phys.*, **41**, 271 (1979).

0002-7863/84/1506-0976$01.50/0

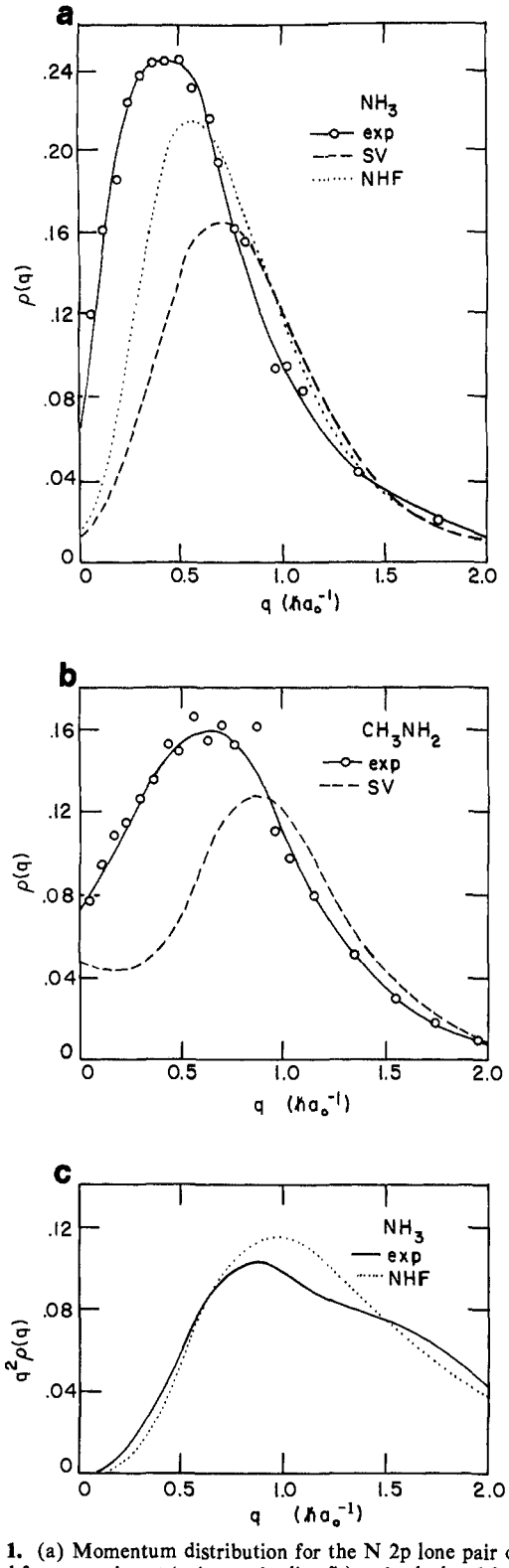

Figure 1. (a) Momentum distribution for the N 2p lone pair of NH_3 obtained from experiment (points and spline fit) and calculated from split valence, SV(---), and near Hartree–Fock, NHF(···), wave functions. (b) Momentum distribution for the lone-pair orbital of CH_3NH_2 obtained from experiment (points with spline fit) and calculated from SV(---) wave function. (c) Momentum radial distribution function $q^2\rho(q)$ from the lone pair of NH_3 from experiment (—) and calculated from NHF(···) wave function.

by analyzing the corrresponding $\Delta B(r)$ functions.[10] To show this type of analysis can yield new information of a chemical nature we examine here the lone-pair orbitals of NH_3 and CH_3NH_2.

(10) J. A. Tossell, J. H. Moore, M. A. Coplan, G. Stefani, and R. Camilloni, *J. Am. Chem. Soc.*, **104**, 7416 (1982).

It is well-known that CH_3NH_2 has a larger proton affinity than NH_3[11] (207 kcal/mol for NH_3 vs. 216–218 kcal/mol for CH_3NH_2). This difference has been attributed to the inductive and polarization stabilization effects of the methyl group.[12] The observed correlation of N lone-pair ionization potentials with proton affinities for the alkylamines has been associated with polarization stabilization of the final-state cation by the alkyl groups.[13] The relative proton affinities of NH_3 and CH_3NH_2 have also been calculated by a number of different groups[14] with SCF–LCAO–MO methods. When small basis sets are used, calculated proton affinities are significantly larger than the experimental values; however, the difference in proton affinity between NH_3 and CH_3NH_2 can be obtained fairly accurately by using even a minimum basis set.[14a,b] The energy and charge distribution decomposition analysis of Morokuma and co-workers[15] has also been employed to interpret the difference between NH_3 and CH_3NH_2 proton affinities. It was found for both split valence[14d] (SV) and larger polarized basis set[14e] calculations that the larger proton affinity of CH_3NH_2 arose almost entirely from a more attractive polarization energy (defined in this case as the energy change resulting from distortion of the electron cloud of the base by the field of the approaching proton). Although the polarization energy comes from rearrangement of the total molecular electron density, it is apparent from calculations that the highest occupied orbital, the N 2p lone pair, is the most strongly polarized by an approaching proton. The admixture of methyl orbital character into this lone-pair orbital in CH_3NH_2 may be qualitatively understood by using perturbational MO theory.[16] Such mixing of methyl π^* orbital character into the N lone pair has been used to explain the tilt angle of the methyl group C_3 axis with respect to the C–N bond axis and is expected to also affect the rotational barrier.

There are thus a number of theoretical studies that have emphasized the importance of methyl orbital admixture. The experimental evidence for these theoretical arguments currently consists of single measurements of ionization potential or proton affinity. The information content of such measurements is low, and they do not provide the rigorous tests necessary to either confirm or reject the theoretical ideas. Single-electron momentum distributions, however, contain a great deal of information about electronic structure and even when spherically averaged can provide useful tests of theory. In this work we present experimental, spherically averaged momentum densities for the lone-pair electrons of NH_3 and CH_3NH_2. Connection between the momentum densities and wave functions is established through $B(r)$, the Fourier transform of the momentum density.

Experimental Section

A discussion of the basic experiment has already been given.[17] To obtain accurate $B(r)$ functions from experimental data requires the reduction of both random and systematic errors to the level of a few percent. For this reason the (e,2e) spectrometer has been modified to (1)

(11) (a) D. H. Aue, H. M. Webb, and M. T. Bowers, *J. Am. Chem. Soc.*, **94**, 4726 (1972); (b) M. T. Bowers, D. H. Aue, H. M. Webb, and R. T. McIver, *J. Am. Chem. Soc.*, **93**, 4314 (1971).

(12) W. G. Henderson, J. L. Beachamp, D. Holtz, and R. W. Taft, *J. Am. Chem. Soc.*, **94**, 4724 (L972).

(13) (a) R. L. Martin and D. A. Shirley, *J. Am. Chem. Soc.*, **96**, 5299 (1974). (b) D. W. Davis and J. W. Rabalais, *ibid.*, **96**, 5305 (1974).

(14) (a) W. J. Hehre and J. A. Pople, *Tetrahedron Lett.*, **34**, 2959 (1970); (b) A. Pullman and P. Brochen, *Chem. Phys. Lett.*, **34**, (1975); (c) A. Johansson, P. A. Kollman, J. F. Liebman, and S. Rothenberg, *J. Am. Chem. Soc.*, **96**, 3750 (1974); (d) H. Umeyama and K. Morokuma, *ibid.*, **98**, 4400 (1976); (e) H. Berthod and A. Pullman, *Isr. J. Chem.*, **19**, 299 (1980); (f) R. A. Eades, D. A. Well, D. A. Dixon, C. H. Douglass, Jr., *J. Am. Chem. Soc.*, **85**, 981 (1981).

(15) (a) K. Morokuma, *J. Chem. Phys.*, **55**, 1236 (1971); (b) K. Kitaura and K. Morokuma, *Int. J. Quantum Chem.*, **10**, 325 (1976); (c) K. Morokuma, S. Iwata, and W. A. Lathan, "World of Quantum Chemistry", R. Daudel and B. Pullman, Ed., Reidel, Dordrecht, Holland, 1974, p 277.

(16) A. Pross, L. Radom, and N. V. Riggs, *J. Am. Chem. Soc.*, **102**, 2253 (1980).

(17) (a) J. N. Migdall, M. A. Coplan, D. S. Hench, J. H. Moore, J. A. Tossell, V. H. Smith, Jr., and J. W. Liu, *Chem. Phys.*, **57**, 141 (1981); (b) J. H. Moore, M. A. Coplan, T. L. Skillman, E. D. Brooks, *Rev. Sci. Instrum.*, **49**, 463 (1978); (c) T. L. Skillman, E. D. Brooks, M. A. Coplan, J. H. Moore, *Nucl. Instrum. Methods*, **159**, 267 (1978).

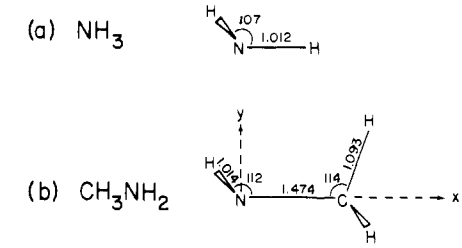

Figure 2. Geometries and orientations assumed for NH_3 and CH_3NH_2 (distances in Å; angles in deg; ∠NCH (in plane) from calculation, ref 24c).

reduce the ambient magnetic field to less than 10^{-4} G with a three-dimensional Helmoltz coil and a double magnetic shield, (2) reduce stray electrons with a positively charged shield, and (3) improve detector calibration through the use of the cylindrically symmetric background. The experimental data have been fitted with cubic spline functions over the region 0–2.0 $\hbar a_0^{-1}$ (an electron with momentum 1.0 $\hbar a_0^{-1}$ has a kinetic energy of 13.6 eV and a wavelength of 2π a_0). The momentum resolution, Δq, was between 0.10 and 0.12 $\hbar a_0^{-1}$, depending upon the ϕ angle.[17a] The data have been normalized to

$$n = \frac{1}{4\pi}\int_0^{2.0\hbar a_0^{-1}} \rho(q) q^2 \, dq \qquad (5)$$

where n is the number of equivalent electrons in the orbital. Points beyond 2.0 $\hbar a_0^{-1}$ were excluded because experimental and theoretical evidence suggests a breakdown of the plane wave impulse approximation above about 2.0 $\hbar a_0^{-1}$, leading to too large values for the cross section.[18]

The vertical ionization potentials obtained by photoelectron spectroscopy for the lone-pair electrons of NH_3 and CH_3NH_2 are 11.0 and 9.6 eV.[19] Separation energy spectra confirmed these values, and momentum distributions were obtained at the appropriate energies.

Results and Discussion

The momentum distributions are shown in Figure 1. Theoretical momentum distributions were obtained for the $3a_1$ lone pair of NH_3 and CH_3NH_2 using the algorithms and program of Epstein[20] (see ref 21 for a more comprehensive treatment). For comparison between the molecules we use the 4-31G split valence (SV) basis.[22] We have also repeated the near Hartree–Fock (NHF) calculations of Rauk, et al.[23] for NH_3. The geometries[24] employed in the wave function calculations are given in Figure 2.

The experimental distribution for NH_3 is similar to that of Hood et al.[6a] but has its maximum at a slightly smaller value of q (0.41 vs. 0.5 $\hbar a_0^{-1}$) and shows a steeper decline as q approaches zero, probably due to the better momentum resolution of the present data.

When a SV basis set is used, the calculated position of the maximum in $\rho(q)$ increases from 0.69 $\hbar_0^{-1}$ for NH_3 to 0.86 $\hbar a_0^{-1}$ for CH_3NH_2. The maxima in the experimental momentum densities are at 0.41 and 0.64 $\hbar a_0^{-1}$, respectively. Since the quantum mechanical operator for momentum is proportional to the gradient in position space, a shift of $\rho(q)$ to higher momentum implies a wavefunction varying more rapidly in position space. The improvement in $\rho(q)$ as the basis set is expanded for NH_3 implies that the SV basis set is not sufficiently flexible to give a good description of the lone-pair electron density. To further investigate the sizeable discrepancy between the experimental data and the near Hartree–Fock level calculations we have plotted the radial momentum density, $\rho(q)q^2$, as a function of q for both

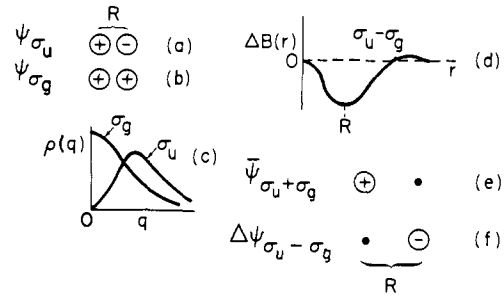

Figure 3. Pictograms illustrating the relationship of $\psi(\vec{r})$, $\rho(q)$, $\Delta B(r)$, $\bar{\psi}(\vec{r})$, and $\Delta\psi(\vec{r})$ for the σ_g and σ_u orbitals obtained by linear combination of s valence orbitals in a homonuclear diatomic molecule.

experiment and theory in Figure 1c. The radial momentum density takes into account the change in the momentum volume element with momentum and is in some ways a more physically meaningful quantity than $\rho(q)$. Interestingly enough, when radial momentum density is considered the apparent discrepancy between experiment and theory is reduced with the largest differences now appearing at intermediate and large momenta. Possible causes include correlation effects and the change in electronic wavefunction with vibrational motion. Also to be considered are distortions of the incoming and outgoing electron waves resulting in a partial failure of the plane wave approximation and inadequacies in the Hartree–Fock basis set which though optimized for total energy may inadequately represent other electronic properties such as the momentum density. Because we are concentrating on differences between NH_3 and CH_3NH_2, there will be some concellation in the discrepancies which in any case do not exceed several percent overall.

To make the comparison between the momentum densities for NH_3 and CH_3NH_2 more quantitative we have first taken the numerical Fourier transform of the calculated and measured momentum densities to obtain $B(r)$ and have then formed the difference function

$$\Delta B(r) = B(r)_{CH_3NH_2} - B(r)_{NH_3} \qquad (6)$$

As we have shown,[7] $\Delta B(r)$ can be approximated as

$$\Delta B(\vec{r}) = \int \bar{\psi}_{ij}(\vec{s})\Delta\psi_{ij}(\vec{s}+\vec{r})\, d\vec{s} + \int \Delta\psi_{ij}(\vec{s})\psi_{ij}(\vec{s}+\vec{r})\, d\vec{s} \qquad (7)$$

where $\bar{\psi}_{ij}(\vec{r}) = 1/2(\psi_i(\vec{r}) + \psi_j(\vec{r}))$ and $\Delta\psi_{ij}(\vec{r}) = \psi_i(\vec{r}) - \psi_j(\vec{r})$.

A graphical representation of this approximation can be used to explain the form of $\Delta B(r)$ as illustrated by the pictograms in Figure 3 for the simple case of the σ_g and σ_u orbitals of a homonuclear diatomic. Pictograms of $\psi_{\sigma_g}(\vec{r})$ and $\psi_{\sigma_u}(\vec{r})$ are given in Figure 3a,b, the corresponding momentum distributions in Figure 3c, the $\Delta B(r)$ function in Figure 3d, and the one-electron wave function average and difference, $\bar{\psi}(\vec{r})$ and $\Delta\psi(\vec{r})$, in Figure 3e,f. One can show algebraically[9] that for this simple case $\Delta B(r)$ has a minimum at a distance equal to the internuclear distance, R. Equivalently, the minimum in $\Delta B(r)$ may be associated with the presence of oppositely signed extrema in $\bar{\psi}(\vec{r})$ and $\Delta\psi(\vec{r})$ which are separated by R. If $\bar{\psi}(\vec{r})$ is known reasonably well we obtain direct information on $\Delta\psi(\vec{r})$, the change in wave function from one case to another, by analyzing $\Delta B(r)$. Such an analysis may of course be hindered by the absence of directional information in $\Delta B(r)$ for unsymmetrical molecules and delocalized orbitals.

In Figure 4a we show the $\Delta B(r)$ functions for the lone-pair orbitals of NH_3 and CH_3NH_2 obtained from SV calculations and from experiment. The fact that the experimental and theoretical functions are similar is good evidence for the accuracy of the experimental results. The $\Delta B(r)$ function may be interpreted by using the $\bar{\psi}(\vec{r})$ and $\Delta\psi(\vec{r})$ maps shown in Figure 4d, e. In the construction of these maps the N atoms of NH_3 and CH_3NH_2 have been placed at the same position, and the N–C bond direction in CH_3NH_2 has been taken coincident with one of the N–H bonds of NH_3. Note that in the most stable CH_3NH_2 geometry one of the H atoms of the methyl group lies in the plane of the illustration which is the plane bisecting ∠HNH. It is apparent from Figure

(18) (a) N. Chant, Department of Physics, University of Maryland, unpublished results; (b) K. T. Leung and C. E. Brion, *Chem. Phys.*, **82**, 87 (1983).
(19) C. Utsunomiya, T. Kobayashi, and S. Nagakua, *Bull. Chem. Soc. Jpn.*, **53**, 1216 (1980).
(20) I. R. Epstein, *Chem. Phys. Lett.*, **9**, 9 (1971).
(21) P. Kaijser and V. H. Smith, Jr., *Adv. Quantum Chem.*, **10**, 37 (1977).
(22) R. Ditchfield, W. J. Hehre, and J. A. Pople, *J. Chem. Phys.*, **54**, 724 (1971).
(23) A. Rauk, L. C. Allen, and E. Clementi, *J. Chem. Phys.*, **52**, 4133 (1970).
(24) (a) NH_3: W. S. Benedict and K. Plyler, *Can. J. Phys.*, **35**, 1235 (1957); (b) CH_3NH_2: T. Nishikawa, *J. Phys. Soc. Jpn.*, **12**, 668 (1957); (c) E. Flood, P. Pulay, and J. E. Boggs, *J. Am. Chem. Soc.*, **99**, 5570 (1977).

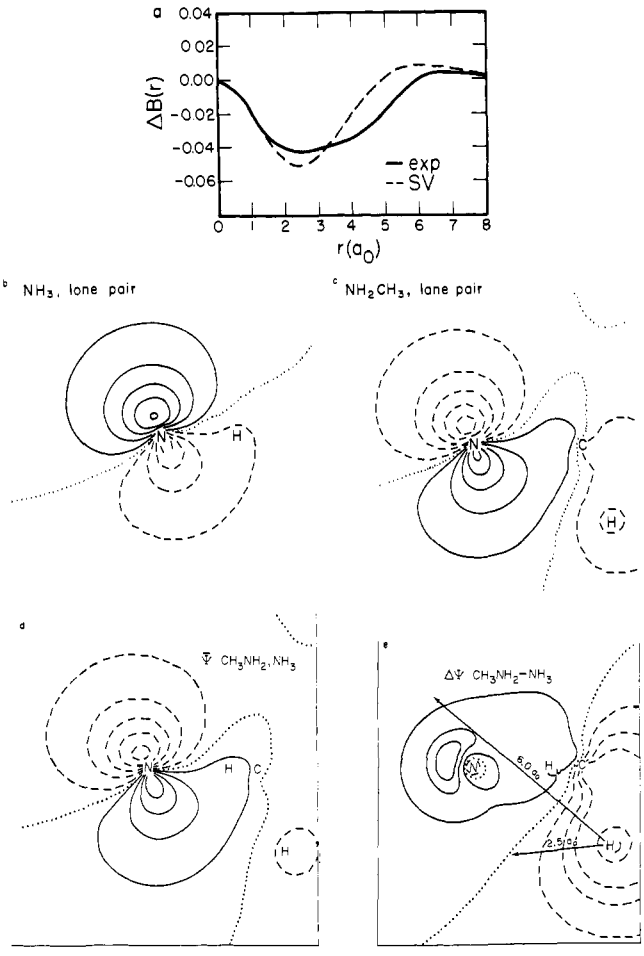

Figure 4. (a) $\Delta B(r) = B(r)_{CH_3NH_2} - B(r)_{NH_3}$. (b) $\bar{\psi}(\vec{r})_{NH_3}$, SV(in plane of N, H, and lone pair). (c) $\bar{\psi}(\vec{r})_{CH_3NH_2}$, SV(in plane of N, C, and H trans to lone pair). (d) $\bar{\psi}(r) = 1/2[\bar{\psi}(\vec{r})_{CH_3NH_2} + \bar{\psi}(\vec{r})_{NH_3}]$. (e) $\Delta\psi(r) = \bar{\psi}(\vec{r})_{CH_3NH_2} - \bar{\psi}(\vec{r})_{NH_3}$. (Positive contours—; negative contours – – –; zero contour •••; $\Delta\psi$ contour values go from +0.08 to −0.38 (electron/$a_0^3)^{1/2}$).

4 b–d that the NH_3, CH_3NH_2, and averaged wave functions are similar, all showing amplitude maxima of essentially p shape above and below the N–H or N–C bonds. One difference between the orbital plots for NH_3 and CH_3NH_2, however, is the presence of a node between the nitrogen and the in-plane H (trans to the major lone-pair orbital lobe) in CH_3NH_2. The node arises from H 1s and C 2p contributions that interfere destructively with the N 2p contributions. Such a node requires a more rapid change in $\bar{\psi}(\vec{r})$ with distance in the CH_3NH_2 case and is thus consistent with the fact that the momentum density for CH_3NH_2 has higher momentum components than that for NH_3. Inspection of the $\Delta\bar{\psi}(\vec{r})$ plot in Figure 4 e shows that the largest difference of the wave functions indeed occurs near the in-plane H of CH_3NH_2. This minimum in $\Delta\bar{\psi}(\vec{r})$ is separated from the maximum of $\bar{\psi}(\vec{r})$ lying below the N–(H,C) axis by about 2.5 a_0, as indicated by the arrow of that length superimposed upon the $\Delta\bar{\psi}(\vec{r})$ map. The minimum near H in $\Delta\bar{\psi}(\vec{r})$ is also separated by about 6 a_0 from the minimum in $\bar{\psi}(\vec{r})$ lying above the N–(H,C) axis, as indicated by a second arrow. Of course, such an interpretation takes into account only one plane passing through the molecule, but since only this (vertical) plane contains the C atom it in fact contains the major element distinguishing NH_3 and CH_3NH_2. Since $\bar{\psi}\Delta\psi$ has not been numerically integrated in this plane, we have tried to estimate the dominant contributions by focusing upon the extrema of $\bar{\psi}(\vec{r})$ and $\Delta\bar{\psi}(\vec{r})$. Nonetheless, it seems that the qualitative difference between the NH_3 and CH_3NH_2 lone-pair orbitals may be adequately explained in terms of C 2p and H 1s admixture in CH_3NH_2. The dominant term seems to be the trans-H 1s, which is antibonding with respect to the N 2p. A similarity of SV and experimental $\Delta B(r)$ plots suggests that such effects occur in the true molecular wave functions as well as in the SV SCF approximations to them.

Conclusion

From high-precision experimental momentum distributions obtained by the (e,2e) technique it has been possible to derive $B(r)$ functions for the lone-pair orbitals of NH_3 and CH_3NH_2. The difference in these functions $\Delta B(r)$ is very similar to a $\Delta B(r)$ calculated from theoretical wave functions and gives confidence in the experimental method. The interpretation of $\Delta B(r)$ in terms of wavefunction averages $\bar{\psi}(\vec{r})$ and differences $\Delta\bar{\psi}(\vec{r})$ is consistent with the participation of C 2p and trans-H 1s orbitals in the lone-pair orbital of CH_3NH_2, but because the conclusions derived from the (e,2e) data are dependent on the availability of theoretical wave functions, the generality of the method is limited. The method does demonstrate, however, that good-quality experimental (e,2e) momentum distributions contain information of sufficient detail about electronic structure to allow for the elucidation of the chemical properties of molecules.

Acknowledgment. This work was supported by the National Science Foundation under Grant No. CHE-8205884 and by the Computer Science Center, University of Maryland.

Registry No. NH_3, 7664-41-7; CH_3NH_2, 74-89-5.